processes

MDPI

Article

Geometallurgical Detailing of Plant Operation within Open-Pit Strategic Mine Planning

Aldo Quelopana [1,2], Javier Órdenes [2], Rodrigo Araya [3] and Alessandro Navarra [2,*]

[1] Department of Systems and Computer Engineering, Universidad Católica del Norte, 0610 Angamos, Antofagasta 1270709, Chile
[2] Department of Mining and Materials Engineering, Faculty of Engineering, McGill University, 3610 University Street, Montreal, QC H3A 0C5, Canada
[3] SNC Lavalin Inc., Mining and Metallurgy, 445 René-Lévesque Blvd. West, Montreal, QC H2Z 1Z3, Canada
* Correspondence: alessandro.navarra@mcgill.ca

Abstract: Mineral and metallurgical processing are crucial within the mineral value chain. These processes involve several stages wherein comminution is arguably the most important due to its high energy consumption, and its impact on subsequent extractive processes. Several geological properties of the orebody impact the efficiency of mineral processing and extractive metallurgy; scholars have therefore proposed to deal with the uncertain ore feed in terms of grades and rock types, incorporating operational modes that represent different plant configurations that provide coordinated system-wide responses. Even though these studies offer insights into how mine planning impacts the ore fed into the plant, the simultaneous optimization of mine plan and metallurgical plant design has been limited by the existing stochastic mine planning algorithms, which have only limited support for detailing operational modes. The present work offers to fill this gap for open-pit mines through a computationally efficient adaptation of a strategic mine planning algorithm. The adaptation incorporates a linear programming representation of the operational modes which forms a Dantzig-Wolfe decomposition, nested within a high-performing stochastic mine planning algorithm based on a variable neighborhood descent metaheuristic. Sample calculations are presented, loosely based on the Mount Isa deposit in Australia, in which a metallurgical plant upgrade is evaluated, showing that the upgraded design significantly decreases the requirement on the mining equipment, without significantly affecting the NPV.

Keywords: open-pit mine planning; metallurgical plant; geometallurgy; stochastic optimization; metaheuristics; linear programming

Citation: Quelopana, A.; Órdenes, J.; Araya, R.; Navarra, A. Geometallurgical Detailing of Plant Operation within Open-Pit Strategic Mine Planning. *Processes* **2023**, *11*, 381. https://doi.org/10.3390/pr11020381

Academic Editor: Haiping Zhu

Received: 4 January 2023
Revised: 20 January 2023
Accepted: 23 January 2023
Published: 26 January 2023

1. Introduction

The design and redesign of a metallurgy plant is not a trivial decision for a mining company since it significantly impacts its mineral value chain. It is known from general system theory that separate-optimized subsystems do not guarantee an entire-optimized system [1]; therefore, the analysis of any change in a plant must be addressed strategically from a holistic point of view by supporting internal optimization and addressing the interdependency between adjacent processes. This challenging decision must consider several risks such as geology complexity (complex geometric shapes of deposits, deep-seated deposits, geotechnical challenges, etc.), lower ore grades, ore quality variability (textural complexities, mineralogical variability, etc.), and large production volumes [2].

Comminution is essential to mineral processing and metallurgical extraction because it liberates the sought-after minerals needed for their subsequent selective recovery through processes such as flotation and leaching [3,4]. However, comminution consumes a considerable amount of energy, in the order of 50–80% of the mine site [5,6], as so much of this energy is dissipated as heat into the rock. Moreover, some decades ago, scholars realized that comminution could consume up to 4% of global electrical energy [7]. The performance and

throughput of the two components of comminution, crushing and grinding, are affected by ore types that are spatially distributed throughout the deposit, in terms of hardness, liberation size and ultimately the metal recovery [8]. Therefore, optimizing comminution performance in consideration of these properties is crucial in balancing production goals, with lower carbon footprints, and reduced energy consumption [9].

Prediction models based on ore hardness have been developed for several well-known mines; for example, the Escondida porphyry copper mine in Chile has used these models—generated based on annual testing programs or drill hole samples—to forecast the throughput and ball mill product size (P80) for each ore block since 2000. These models have delivered estimates of two main descriptions, the Bond Work Index (BWi) and the SAG power index [10], being the first the most widely used [11]. This index is expressed in kWh and is calculated using a standard procedure introduced by Bond [12]. It is highly influenced by geological features, specifically by lithology and mineral composition, which is the reason why Haffez [13] compared this index versus the mechanical properties of ores hosted in rock with different formations (bauxite, kaolinite, granodiorite, magnetite, granite, and quartz). He concluded that BWi is positively related to hardness (R^2 = 0.75), which strongly influences this correlation with mineralogical composition, specifically with quartz content.

A key difference that distinguishes the mineral value chain from other value-adding systems is the geological uncertainty, which is a significant factor in cost overruns [14]. The plant must deal with the chance of being fed with rock types that possess different grades than expected, trying to maximize the profit by prioritizing them in some manner. To deal with significant and sustained changes in the provided ore (with different hardness), the concept of operational modes was presented by Navarra et al. [15]. These modes are expressed in parameters that summarize alternate plant configurations to respond efficiently to what combination of ores are being received. They are the result of adding new processing equipment or technology investments. The mentioned study [15], along with others subsequently published [16–18], provides essential insights related to how mine planning (an adjacent previous process) impacts the ore supplied into the metallurgical plant; however, they do not optimize both under the same framework, which causes a lack of representation of the transitionary periods in the mine life, in which balances of rock types are supported through the strategic alternation of these modes. Of course, strategic mine planning has been studied frequently since the 1960s, providing essential contributions to mine operations [19,20], formulated as a maximization of the net present value (NPV) that determines which blocks should be extracted during each period within the life of the mine [21]. In recent decades, much emphasis has been placed on managing geological uncertainty (especially grade), through stochastic optimization, as will be described in the following section [14,22].

This study aims to present a simultaneous optimization of a system composed of the mine planning and the metallurgy plant, which incorporates different types of ore and geological uncertainty. Unlike previous approaches, the new formulation supports modes of operations with the increased resolution of geometallurgical considerations; most notably, the new approach avoids the previous metaheuristic tuning parameters and soft constraint violations which do not have a true interpretation in the mining context, and which have masked over the intended detailing of mineral and metallurgical operations. This novel approach is applied to a case study loosely based on the Mount Isa operations in Australia, which possess a Zn-Pb orebody.

2. Advances in Stochastic Open-Pit Mining Algorithms

An orebody may be conceived as a discretized set of geometallurgical units called mine blocks. These models are developed considering various ore characteristics such as mineralogy, liberation, texture, and mineral chemistry [18]. Due to the expensive nature of obtaining drill core samples to analyze such factors, geostaticians have proposed diverse methods to understand and improve confidence in the spatial distribution of these

characteristics, especially in the volumes between measured sample points. This allows for the improved delineation of distinct domains (i.e., groupings of blocks) based on the expected metallurgical response as a function of the inherent geological characteristics; these distinct domains are often called "geomatellugical units". Kriging is a well-known approach for spatial interpolation, and is commonly applied in strategic mine planning that is based on deterministic optimization; indeed, kriging provides one single scenario, often hypothesized as the "most likely scenario", and resulting (deterministically) optimum overly adheres to this one scenario, and is thus poorly adapted to the actual geological variations that are manifest within the life of mine. Moreover, this one scenario that is produced by a typical kriging approach is not actually likely and is criticized as being overly smoothed; this is problematic for high-grade ore that is adjacent to waste rock since this smoothening will cause the ore to be "smudged out" within the model, or otherwise cause an erroneous volume of low-grade ore. The countervailing approach has been, rather than using kriging to produce a single (overly smoothed) scenario subject to deterministic optimization, has been to apply a form of Monte Carlo simulation known as conditional simulation, which produces countably many equiprobable scenarios that are then subject to stochastic optimization. The most common form of conditional simulation is Sequential Gaussian Simulation [23], which can be seen as a logical extension of kriging. Nonetheless, the resulting stochastically optimized mine plan is not overly adherent to any of the equiprobable scenarios but rather is expected to perform well for the entire distribution of possible scenarios. The objective is to maximize the expected net present value over these scenarios. Thus, by simultaneously incorporating a range of equiprobable scenarios (typically between 10 and 20), the stochastic approaches address critical aspects of geological variability, which are inherent to large mining projects.

While the stochastic approaches are gaining prominence, many advances in open pit mine plan algorithms have been presented within deterministic formulations, i.e., considering one single scenario, rather than a simultaneous consideration of multiple scenarios. It is not intended to provide a comprehensive summary; however, among these studies are methodologies that are highlighted to generate operational ramps [24], an aggregation-disaggregation heuristic applied to the mine block sequencing problem [25], an efficient computing of ultimate pit limits [26], and strategic open-pit mine planning based on a mixed-integer approach with the Bienstock and Zuckerberg method [27]. Nevertheless, without detracting from the merit of the mentioned studies, it has been proved that managing risks of at least ten scenarios increases the accuracy of the results and the expected net present value of projects by as much as 25% [14,22]. It is noteworthy that each of these "deterministic" developments could be adapted into a multi-scenario stochastic which may, in practice, be quite important in addressing the geological uncertainty, especially in grades and rock types. Yet, specifically under the stochastic methods, different complexities have been addressed to add realism to the calculations, among which it is found stockpiling [28], balancing output from multiple pits [29], multiple processing streams [30], and market uncertainty [31]. These studies have generally tackled the strategic and tactical levels [32].

Due to the shear size of the problem, e.g., with many thousands or millions of blocks, it is challenging from a computational-capacity perspective to construct optimal solutions to realistic study cases through exact methods such as the Simplex Method. Therefore, several studies have relied on metaheuristics even though they did not guarantee an optimum. Some examples of these optimization algorithms are Simulated Annealing [33], Tabu Search [34], or Particle Swarm Optimization [35]. The acceptance of heuristics as an alternative to exact is partly due to the relative sizing of this optimization uncertainty, in comparison to the inherent geological uncertainty. Nevertheless, the main drawback of these heuristics is their reliance on tuning parameters that control the optimization process, which can significantly impact the method's effectiveness. For example, in comparing two designs at a mine, one may evaluate an option with unintentionally favorable tuning values and then assess the second design with unintentionally unfavorable ones. Moreover,

adjusting these parameters adds extra time to finding an acceptable solution because it implies the repetition of the experiments.

One solution that avoids these tuning parameters is the Bienstock-Zuckerberg (BZ) algorithm, a specialized linear programming technique that relies on matrix decompositions. Relevant studies have implemented it in the mine planning context; however, these contributions have resided within a deterministic approach [27,36] and have not yet been extended to consider plant operations. Another exception is the Variable Neighborhood Descent (VND) metaheuristic, initially proposed by Lamghari et al. [21,37], which is formulated to avoid ambiguous parameters and work under stochastic contexts. Moreover, it has been found to be remarkably well-suited for parallel computing. Due to these characteristics, the VND algorithm has been part of a series of publications seeking to optimize the stochastic strategic mine plan along with metallurgy plants [16–18]. These studies define and use the concept of operational modes; however, they do not depict the tactical alternation of modes in response to the geological scenario, thus limiting the geometallurgical detailing. The present work advances this matter by imbedding a linear programming formulation within the VND heuristic, which is to be evaluated as a response to each scenario; as with other open-pit stochastic algorithms, it produces one single mine plan that confronts an enumerated set of 10–20 scenarios; however, the assessment of the plan under each scenario constitutes a separate linear program.

3. Formulation

3.1. First Stage Optimization—The Overarching Strategic Plan

The VND algorithm originally developed by Lamghari et al. [21], and then later adapted by Navara et al. [16–18] to support operational modes, is now further extended to detail these operational modes in response to short-term (tactical) geometallurgical considerations. These stochastic formulations [16–18,21,23,33,34,37] each conform to what is generally known as Two Stage optimization. The first stage may be called the "strategic" or "long-term" stage, which determines the blocks to be excavated and fed into the plant in each period, thus forming the long-term mine plan; this strategic formulation produces one single mine plan that confronts the set of equiprobable scenarios, without yet knowing which precise scenario will actually manifest. The second stage of optimization represents the shorter-term processing decisions of how the ore will be processed after the knowledge of the geological scenarios; this second stage constitutes a separate optimization for each of the scenarios and is developed in Section 3.2.

Let $\mathcal{B}$ is the set of blocks within the scope of the optimization, and n_S and n_T to be the number of geological scenarios and time periods, respectively. From this, the mine plan is expressed as $x = \{\mathcal{B}_t\}_{t=1}^{n_T}$ in which $\mathcal{B}_t \subset \mathcal{B}$ is the set of blocks to be mine in time period t. As with the original work of Lamghari et al. [21], strategic stockpiles are not considered, so a block $b \in \mathcal{B}_t$ that is mined in period t can only be processed in t. However, this decision of ***if*** the block should be processed depends on the geological scenario; in some scenarios, the block will be ore and will thus be processed, whereas in other scenarios, the block may be waste rock and therefore rejected. Beyond this question of ***if***, the new formulation now considers ***how*** the content of the block will be processed, which again depends on the geological scenario; thus, in some scenarios, the block may be most amenable to operating mode A, but in other scenarios, it may be more amenable to mode B, and still in other scenarios it may be waste rock. For simplicity, the current set of calculations will consider only two modes, which already support significant geometallurgical complexity, as demonstrated in Section 4; the formulation is directly extendible to more modes.

The objective is to maximize the expected NPV, as expressed by

$$\max[f(x)] = -\sum_{t=1}^{n_T} \sum_{b \in \mathcal{B}_t} c_{bt} + \frac{1}{n_S} \sum_{s=1}^{n_S} \sum_{t=1}^{n_T} f_{st}(\mathcal{B}_t) \quad (1)$$

in which the first double summation considers the discounted cost of mining block b in period t, denoted c_{bt}; these mining costs are incurred independently of the geological scenario. The rightmost double sum constitutes the expected discounted revenue attained from processing the blocks, which is indeed dependent on the geological scenarios. The double sum is preceded by $(1/n_S)$ since it is fact a scenario-wise average of a life-of-mine summation. In this, $f_{st}(x)$ is the discounted value attained under scenario s, in period t, given mine plan x. As will be developed in Section 3.2, and Appendix A, $f_{st}(x)$ is itself the result of an optimization, i.e., the aforementioned second stage.

For a proposed mine plan $x = \{\mathcal{B}_t\}_{t=1}^{n_T}$ to be feasible, it must satisfy the following constraints,

$$\bigcup_{b \in \mathcal{B}_t} \mathcal{B}_b^{Pred} \subseteq \bigcup_{t'=1}^{t} \mathcal{B}_{t\prime}, \quad \forall t \in \{1, \ldots, n_T\} \tag{2}$$

$$\sum_{b \in \mathcal{B}_t} m_b \leq M_t, \quad \forall t \in \{1, \ldots, n_T\} \tag{3}$$

in which $\mathcal{B}_b^{\text{Pred}}$ is the set of direct predecessors of block b, i.e., the set of blocks $\mathcal{B}_b^{\text{Pred}}$ must be mined in order to give access to b through a not overly steep slope. Within Equation (3), m_b denotes the mass of block b, and M_t is the maximum mass of rock that can be mined during period t, i.e., the mining capacity.

The technical details of the VND algorithm are described in previous work [16–18], and shall not be revisited recounted here, except to note that blocks are transferred between periods, either through trading a single block with another block from another period (swapping action) or through the shifting cone-shaped groupings of blocks, be it to expedite the grouping (shift-before action) or to postpone the grouping (shift-after action). For a solution $x = \{\mathcal{B}_t\}_{t=1}^{n_T}$, each of these transferring actions define a different set of neighboring solutions, hence the phrase "variable neighbourhood". The algorithm iteratively searches for neighbors having higher expected NPV, which can be considered as an "ascent", but the VND metaheuristics were originally conceived for minimization, hence the term "descent". Throughout each iteration, the algorithm never allows a block to be mined in more than one period. Hence, a feasible solution $x = \{\mathcal{B}_t\}_{t=1}^{n_T}$ must satisfy,

$$\mathcal{B}_t \cap \mathcal{B}_{t\prime} = \varnothing, \quad \forall t, t' \in \{1, \ldots, n_T\} \tag{4}$$

which is often called the reserve constraint. Thus, the first stage of optimization can be understood as a constrained optimization to maximize the expected NPV (Equation (1)), while satisfying block precedence, mining capacity and reserve constraint, as specified by Equations (2)–(4), respectively. There is, however, a subtlety in Equation (1) since f_{st} constitutes n_S conditional short-term optimizations that are embedded within the strategic optimization.

3.2. Second Stage Optimization—The Short-Term Processing Decisions

The short-term decisions are to partition the mass m_b of each mined block $b \in \mathcal{B}_t$ among the various processing modes that are available, or potentially to reject some or all of the mass as waste rock. As per the formulation of Equation (1), the scope of the short-term optimization assumes a static set of blocks is fixed to one single scenario s and one single period t. Furthermore, while the block sets $\mathcal{B}_t$ are being modified by the first-stage (strategic) optimization, these sets are static in the scope of the short-term optimization. The operational question is then posed: "given that these blocks $\mathcal{B}_t$ which we now know to be described by geological scenario s, must be processed within the current period t, how will they best be processed given the limited plant capacity?"

Given a set of operational modes $\mathcal{O}$, the short-term decision variables are m_{bso} which denotes the mass of block b that, under scenario s, will be subject to processing mode o, for each $o \in \mathcal{O}$. These short-term decision variables are subject to the linear objective function,

$$f_{st}(\mathcal{B}_t) = \max \sum_{b \in \mathcal{B}_t} \sum_{o \in \mathcal{O}} \left(\frac{v_{bso}}{m_b} \right) m_{bso} \tag{5}$$

in which v_{bso} is the discounted recoverable value of block b when undergoing processing mode o. This value incorporates considers the grade and rock type, as in previous formulations [16–18]. However, it now considers the broader context of the mode, including the quantity and type of other rock types with which it is combined. Essentially, each mode is designed for a combination of rock types and is able to extract more or less value from each of the feed components. Thus, the constraints consider an available set of modes $\mathcal{O}$, in relation to the rock types $\mathcal{P}$ that may constitute ore; $\mathcal{B}_{\mathrm{ps}} \subset \mathcal{B}$ denotes the set of blocks that under scenario s are of rock type p.

The objective of Equation (5) is thus subject to the constraints

$$\sum_{o \in \mathcal{O}} m_{bso} \leq m_b, \ \ \forall b \in \mathcal{B}_t \tag{6}$$

$$\sum_{o \in \mathcal{O}} \sum_{b \in \mathcal{B}_t} \frac{m_{bso}}{r_o} \leq d_t, \ \ \forall r_o > 0, \ t \in \{1, \ldots, n_T\} \tag{7}$$

$$\sum_{b \in \mathcal{B}_{ps} \cap \mathcal{B}_t} m_{bso} - w_{op} \sum_{b \in \mathcal{B}_t} m_{bso} = 0, \ \ \forall o \in \mathcal{O}, \ \forall p \in \mathcal{P} \tag{8}$$

$$m_{bso} \geq 0, \ \ \forall b \in \mathcal{B}_t, \forall o \in \mathcal{O} \tag{9}$$

in which r_o is the tonnage processing rate mode o, d_t is the available time of plant during the period, and w_{op} is the weight fraction of rock p that is included in the feed for operating mode o. Equation (6), in conjunction with the non-negativity constraints (Equation (9)) specify the problem as a continuous partition of the mass m_{b}, in which the $(|\mathcal{O}|+1)^{\mathrm{th}}$ mode is to treat the mass as waste rock; this relates to a non-negative slack variable that can be inserted into Equation (6) to convert it into equality. Equation (7) describes the processing capacity, considering that each mode can have a different rate limitation, be it from comminution, a part of the separation process, tailings treatment, etc.; to support different net processing rates r_{o}, the plant capacity is quantified in terms of time availability, e.g., if period t consists of one year 8760 h, then d_{t} may be 8000 h to signify that ~10% of the time is devoted to maintenance.

Equation (8) is a linearization of equality,

$$w_{op} = \frac{\sum_{b \in \mathcal{B}_{ps} \cap \mathcal{B}_t} m_{bso}}{\sum_{b \in \mathcal{B}_t} m_{bso}} \quad \forall o \in \mathcal{O}, \ \forall p \in \mathcal{P} \tag{10}$$

which characterizes the feed composition for each mode of operation. Future implementations may consider a range of compositions $[w_{op}^{min}, w_{op}^{max}]$ for each mode, as in

$$w_{op}^{min} \leq \frac{\sum_{b \in \mathcal{B}_{ps} \cap \mathcal{B}_t} m_{bso}}{\sum_{b \in \mathcal{B}_t} m_{bso}} \leq w_{op}^{max} \quad \forall o \in \mathcal{O}, \ \forall p \in \mathcal{P} \tag{11}$$

which can also be linearized, but constitutes not one, but two constraints; moreover, they would be inequalities rather than equalities. However, the current formulation that enforces a strict composition for each mode has a particular appeal as a simple application of the Dantzig-Wolfe (DW) decomposition, which is further described in Appendix A; Equation (8) allows each block of constraints to be one single equation so that the DW subproblems are trivial to resolve. Implementing ranges of compositions, or other complexities requires special programming efforts, including careful management of data structures [18].

A major challenge in embedding the linear program of Equations (5)–(9), is that there are $n_S \times n_T$ running programs which must be updated at each iteration of the VND algorithm. The approach is always to reoptimize the modified linear program as blocks are entering and leaving $\mathcal{B}_t$, rather than reinitializing at every iteration. In general, further development of specialized data structures allows open-pit strategic mine planning to accommodate more complexity while maintaining practical computations times [18]. This is an ongoing area of research.

3.3. Summary of Sets and Parameters

To apply the formulation described by Equations (1)–(9), to construct a mine plan with n_T time periods, in consideration of n_S geological scenarios, it is necessary to define the following sets:

- $\mathcal{B}$ the set of all blocks within the scope of the simulation.
- $\mathcal{B}_b^{\text{Pred}}$ is the set of direct predecessors of block b.
- $\mathcal{O}$ is the set of available operational modes.
- $\mathcal{P}$ is the set of rock types.

Obtaining $\mathcal{B}_b^{\text{Pred}}$ from $\mathcal{B}$ typically requires a specification of the maximal permissible slope that would maintain geomechanical stability. In the following computations, we consider a 45° maximum slope which for each non-surface block b, causes $\mathcal{B}_b^{\text{Pred}}$ to be the overlying block as well as the surrounding eight blocks (hence $| \mathcal{B}_b^{\text{Pred}} | = 9$ for all non-surface blocks).

At the level of the first-stage optimization, each block is characterized according to:

- c_{bt} is the expected discounted cost of mining block b in period t.
- m_b is the mass of block b.

Typically, c_{bt} considers the amount of rock within the block, as well as a discount rate, and is computed as part of a preprocessing step. The second-stage optimization considers the following parameters, listed in alphabetical order:

- d_t is the availability of the plant during the same period t of the set of blocks $\mathcal{B}_t$.
- r_o is the tonnage processing rate under operational mode $o \in \mathcal{O}$.
- v_{bso} is the discounted value of block b by operational mode $o \in \mathcal{O}$ under scenario s.
- w_{op} is the fraction of rock $p \in \mathcal{P}$ needed to process ore under operational mode $o \in \mathcal{O}$.

The plant capacity is described by the combination of d_t and r_o as implemented in Equation (7). Each operating mode $o \in \mathcal{O}$ is described by its processing rate r_o and feed composition.

Conditional simulation is applied to obtain n_S geological scenarios, wherein the grades and rock type of each block is determined for each of the scenarios, as well as any other geological attributes that are used in computing v_{bso}. The sets and parameters summarized in this section allow the current formulation to support fairly demanding geometallurgical detailing, as demonstrated by the following sample calculations.

4. Sample Calculations

4.1. Case Study

The previous section's algorithm is to optimally evaluate a metallurgical plant fed according to a mine plan that maximizes the expected life-of-mine NPV. In this case, the plant design consists of flotation facilities to produce sulfide concentrate from a fictional Zn-Pb deposit, loosely based on the clastic-dominated (CD) deposit observed in the Mount Isa operation in Australia [38]. This deposit possesses a subtype of sediment that hosts Zn-Pb mineralization which occurs as carbonate replacement within a sedimentary rock sequence, which can be hosted in turn in shale, sandstone, siltstone, or mixed clastic rocks [39].

The CD Zn-Pb deposits arise in back arcs and continental rifts, passive margins, and sag basins, which in some cases are tectonic settings that are transitional to one another. Specifically speaking about the CD deposits in the North Australian craton, the Mount Isa

province has continental rift-hosted deposits presented in a deep-water turbiditic basin in the east developed during incision and granite emplacement to the west [40]. Most Zn-Pb-Ag ores in the North Australian zinc belt are hosted by rocks of the Isa super-basin (deposited between 1655 and 1635 Ma) and interpreted as continental sag-hosted deposits [41].

The Proterozoic Urquhart Shale Formation presents three world-class base metal deposits of Mount Isa, Hilton, and George Fisher, which collectively have a pre-mining resource of >370 Mt. (10 wt% Zn, 5.6 wt % Pb, and 120 g/t Ag) [42]. In the Mount Isa deposit, the orebodies were formed by hydrothermal replacement and dilation of the Urquhart Shale. The stratiform Zn-Pb orebodies are located at least 100 m up-dip from the Paroo fault, with the highest grades of Zn-Pb mineralization coinciding with the hinges and short limbs of folds [43]. Mineralization and associated silica-dolomite alteration seem to show combined effects of deformation that resulted in the easterly-dipping (40–50°) Eastern Creek Volcanic abutting a steeply (60–70°) west-dipping Urquhart Shale (Figure 1) [44].

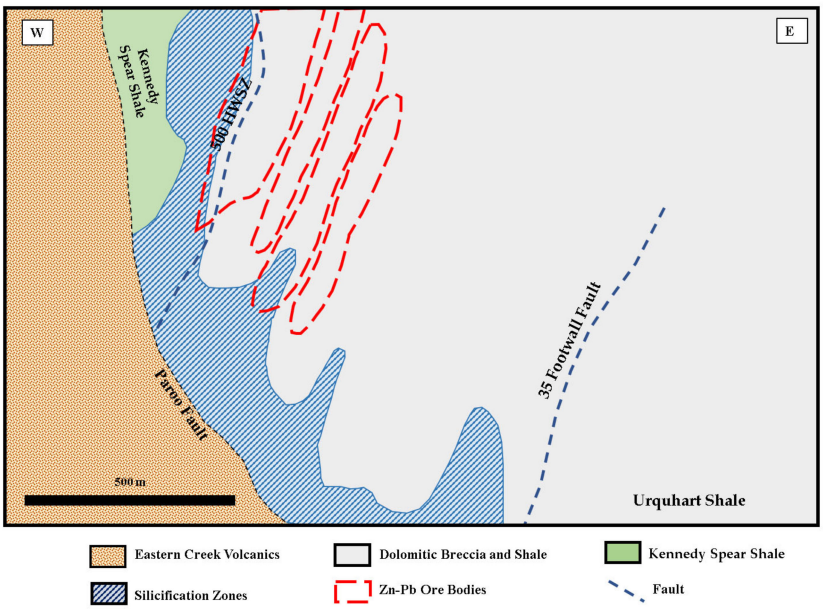

Figure 1. Geological sections showing the distribution of silica-dolomite, Zn-Pb mineralization. Based on the geology of the Mount Isa deposit, silica alteration's geometry is presented as well as its relation to bedding and faults (is a schematic representation, after [44]).

Galena and sphalerite are the dominant Pb and Zn minerals. They occur as stratiform bands that replace stratabound fine-grained pyrite-rich and/or dolomitized shale layers or as infills around highly deformed carbonaceous shale [45]. The Urquhart Shale is siliceous to dolomitic, variably pyritic, and carbonaceous. Several sedimentary facies have been identified in the Urquhart Shale Formation, generally linked to sabkha or playa environments [46].

The CD Zn-Pb pattern observed in Mount Isa was used as guidance to create a block model with twenty scenarios to capture the geological uncertainty; for the purposes of the computation, the scenarios are presumed to be equiprobable, each with different grades. Two main ore types were created (1) a recrystallized dolomite shale sequence, dolomitic breccias to near-massive crystalline dolomite, and (2) high silica in which crystalline dolomite is minor to absent [44]. This model follows the geometry of the folded sequence, dipping west (Figure 1). A schematic profile of the inputted geology is shown in Figure 2.

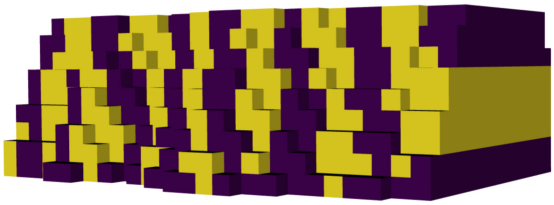

Figure 2. Section of the orebody. Dolomitic Breccia and Shale (yellow)/High Silica Zones (purple).

The geological characteristics and Bond Work Index (BWi) values were assigned based on the study by Nad and Saramak [4] conducted on similar rocks to those found in Mount Isa. These scholars developed a comparative analysis of the strength distribution for irregular particles of carbonates (averaging 9.86 kWh/t) and shale (averaging 15.83 kWh/t), and sandstone ore (with 16.9 kWh/t). The outcomes of this study showed that the most significant amount of energy is required for sandstone-grain grinding due to these particles being predominantly quartz. In those blocks associated with dolomitic shale, the BWi value assigned was 12.85 kWh/t (average of shale and carbonates), whereas, for the high silica, the given value was 16.9 kWh/t.

The metal content of the twenty equiprobable scenarios that were generated for this study are described in Table 1. The variation between the scenarios is indicative of the uncertainty that resides spatially between the drill core sample. A higher density of drill core samples, and/or a less variable orebody, would tend to make each of the scenarios more closely related to a central tendency, which would be observed by smaller standard deviations, or smaller interquartile differences (Q3−Q1). As a consequence, increasing the sampling density will also tighten the interquartile difference in the resulting economic risk profiles, e.g., in the cumulative NPV profiles that will be presented below. However, there is a diminishing return on increasing the sample density, as the underlying variation of the orebody cannot be eliminated and would represent an increasing portion of the total variation. (The limited strategic payoff for successively increasing sampling density can be the subject of a future case study that features intricate budgeting decisions, from a geometallurgical perspective).

Table 1. Descriptive statistics for metal content of the stochastically generated geological scenarios.

	Zn (Tonnes)					Pb (Tonnes)				
Scenario	**Mean**	**Std Dev**	**Q1**	**Median**	**Q3**	**Mean**	**Std Dev**	**Q1**	**Median**	**Q3**
1	1089.84	789.48	503.02	874.05	1471.70	408.90	334.29	165.05	307.99	554.64
2	1065.58	802.90	490.57	831.72	1431.85	399.23	341.90	160.44	291.20	537.72
3	1066.58	798.24	470.64	851.64	1471.70	399.77	338.29	153.11	299.09	554.64
4	1054.75	796.90	460.68	844.17	1429.36	394.79	339.05	149.45	296.12	536.66
5	1047.28	755.80	473.13	864.09	1424.38	390.75	318.87	154.02	304.03	534.55
6	1129.73	860.30	478.11	874.05	1538.93	427.08	367.37	155.85	307.99	583.34
7	1046.75	750.92	490.57	854.13	1409.44	390.38	316.45	160.44	300.07	528.23
8	1077.67	822.96	508.00	861.60	1451.77	404.56	353.03	166.89	303.04	546.17
9	1047.57	767.57	475.62	831.72	1434.34	391.33	323.64	154.94	291.20	538.78
10	1035.72	738.17	478.11	826.74	1404.46	385.57	310.60	155.85	289.23	526.12
11	1081.10	814.24	470.64	851.64	1476.68	406.10	345.77	153.11	299.09	556.76
12	1107.90	811.53	490.57	881.52	1504.07	416.81	344.77	160.44	310.96	568.44
13	1072.85	782.07	500.53	864.09	1429.36	401.63	331.94	164.13	304.03	536.66
14	1107.11	825.36	478.11	859.11	1523.99	417.12	349.74	155.85	302.05	576.95
15	1077.66	793.25	483.09	866.58	1479.17	403.93	337.19	157.69	305.02	557.82
16	1053.30	794.65	468.15	811.80	1426.87	394.28	336.59	152.19	283.34	535.61
17	1076.01	752.17	500.23	874.05	1511.54	402.39	316.13	164.13	307.99	571.63
18	1097.92	802.02	498.04	891.48	1484.15	412.50	340.20	163.20	314.93	559.94
19	1065.79	781.99	480.60	851.64	1461.74	399.06	330.46	156.77	299.09	550.41
20	1076.53	779.98	485.59	888.99	1491.62	403.24	330.09	158.60	313.94	563.13

The computations consider that a nearby plant is being refurbished, possibly upgraded, as part of a longer-term hub-and-spoke strategy that will initially develop the deposit depicted in Figure 2, and eventually several other nearby sites. The plant was originally designed for a 60–40 blend of Dolomitic Shale v/s High Silica ore. However, the deposit is now forecast to provide an imbalance in the two ore types, such that every successive period will require more and more mining in order to feed the plant with the required Dolomitic Shale. A mining rate of roughly 6 Mt/year would be favorable, but apparently, this can only be sustained in the first year. Therefore, a potential upgrade of the plant is under consideration, focusing mainly on the comminution circuit to support an additional operating mode ("Mode B") that will support a 60–40 blend. The cost of the upgrade is still uncertain, and will require detailed designing, outsourced to an engineering firm, and may be as low as $30 M and high as $70 M. However, it is clear that the operating costs for the new Mode B are higher than the existing mode ("Mode A"), since its feed will have a BWi that is proportionately closer to that of sandstone. Table 2 presents the parameters for the existing and upgraded plant designs, including a 16% higher processing cost. A mine capacity of 10 Mt/year was left deliberately high to allow the algorithm to determine that parameter freely and effectively to deactivate Equation (3). For simplicity, the removal of overburden that would lay atop the orebody has not been considered since, although it would be a significant cost in practice, it would be an equal consideration for both plant design options, and therefore irrelevant to the net comparison. Additionally, the data was simulated such that an average of 50% of the mined material is rejected as waste rock, i.e., through an ore sorter.

Table 2. Parameters of the case study are divided into existing and updated plant designs.

Parameters	Existing	Upgraded
Block weight (tonne)	20,000	20,000
Number of blocks	4446	4446
Block dimension (m)	25 × 25 × 12.5	25 × 25 × 12.5
Block density (tonne/m^3)	2.88	2.88
Number of periods	4	4
Length of periods (year)	1	1
Discount rate (%)	8	8
Metal price Zn ($/tonne)	2400	2400
Metal price Pb ($/tonne)	2000	2000
Mining cost ($/tonne)	14.50	14.50
Rejection rate	50%	50%
* Mining capacity (tonne/period)	10,000,000	10,000,000
Processing availability (hr./period)	8059	8059
Rock Types	Dolomitic Shale (D) High Silica (HS)	
Operational Mode A		
Processing cost ($/tonne)	29.15	29.15
Recovery Zn (%)	0.85	0.85
Recovery Pb (%)	0.62	0.62
Processing rate (tonne/hr.)	368	368
Percentage rock D	60	60
Percentage rock HS	40	40
Operational Mode B		
Processing cost ($/tonne)	N/A	34
Recovery Zn (%)	N/A	0.87
Recovery Pb (%)	N/A	0.63
Processing rate (tonne/hr.)	N/A	334
Percentage rock D	N/A	40
Percentage rock HS	N/A	60

* Note that only 50% of the mined material passes through the ore sorter.

4.2. Results

The algorithm was implemented in C++ and ran on a server with a processor Intel® Xeon® CPU E5-2650 using twenty-four threads for parallelization. As mentioned, twenty scenarios were considered: ten for generating an optimized mine plan and the other ten for obtaining risk profiles of the cumulative NPV. Figure 3 shows the curves associated with both designs, where it is natural to observe that the upgraded plant has a higher operational NPV due to it having an additional degree of freedom, i.e., an additional mode. However, this increased revenue of $77 M observed between the two P50 curves is small compared to the impact of geological uncertainty, as measured by the differences between the P10 and P90 curves ($128 M in the case of the existing plant, and $129 M for the upgraded). Moreover, the upgrading costs of $50 ± 20 M are insignificant compared to the geological uncertainty and will be offset by the increase in the revenue of ≈$77 M.

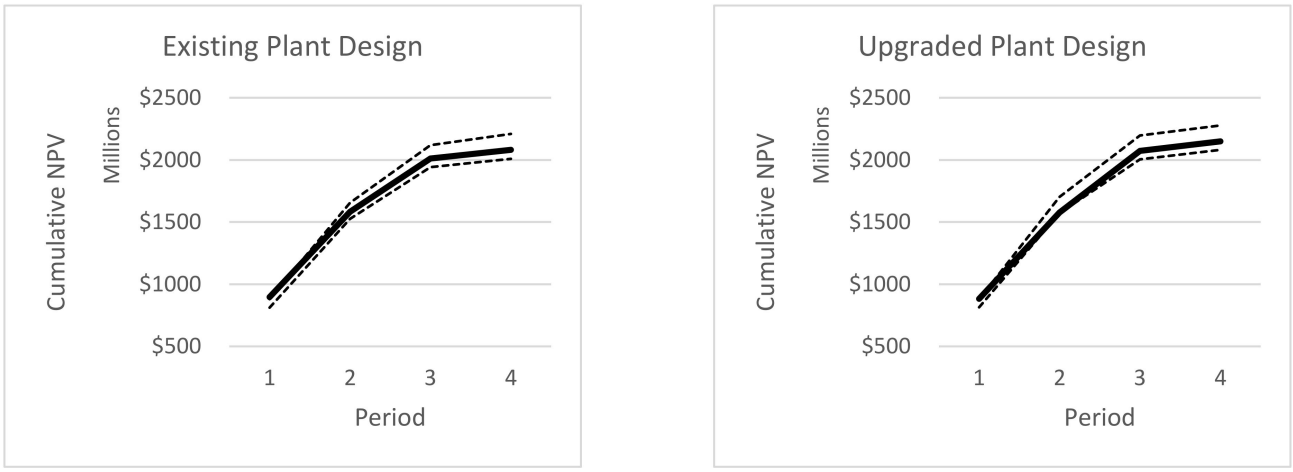

(**a**) (**b**)

Figure 3. P10, P50, and P90 curves cumulative NPV of the existing (**a**) and upgraded (**b**) designs.

More critical for the given context is Figure 4a, which shows how the existing design requires an increasingly higher mining rate in order to keep its only operation mode running. In contrast, the upgraded design stabilizes rock extraction to slightly over 6 Mt/year (Figure 4b). Figure 5a shows the existing plant would attain a throughput of 3 Mt/year operated in the first three years, which corresponds to full capacity considering a plant availability of 8059 h/period and a processing rate of 368 t/h (Table 2). The upgraded plant would is also at full capacity in the first three years, although it is not apparent from Figure 5b; in each of the three first periods, the upgraded plant processes less total ore than the existing plant, considering that a portion of the annual production is carried under Mode B having a slower rate of 334 t/h. Indeed, the upgraded plant is consistently accepts more HS feed than the basic plant, even though the total throughput is lower (Figure 5).

Figure 6 shows the time distribution of the upgraded plant over the four periods for each mode, noting that the existing plant would devote all of its available productive hours to Mode A. Throughout the four periods, Mode B occupies an increasingly large portion of time, and finally dominates in the final period.

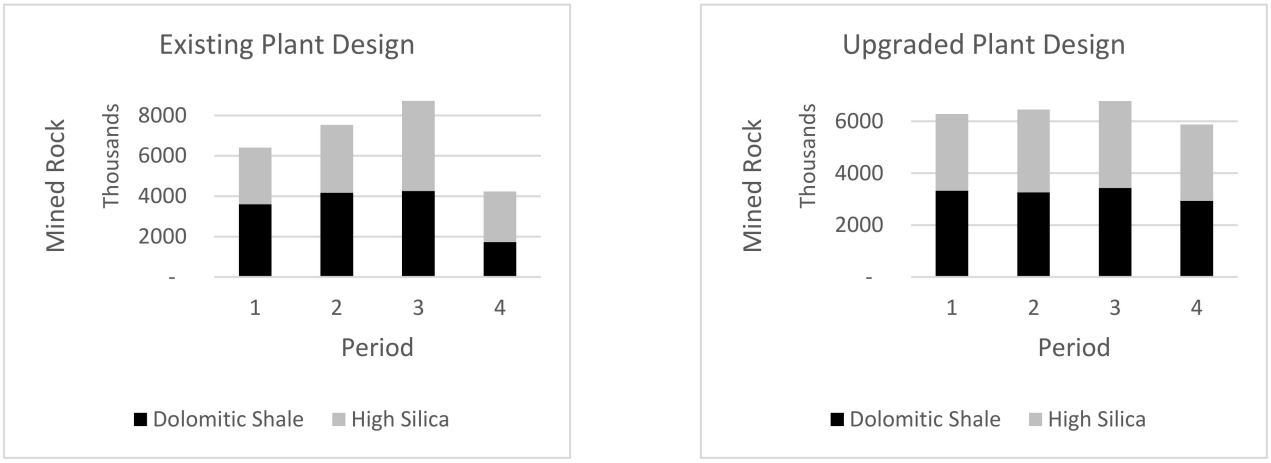

(**a**) (**b**)

Figure 4. Tonnes of rock mined per period for the existing (**a**) and upgraded (**b**) designs.

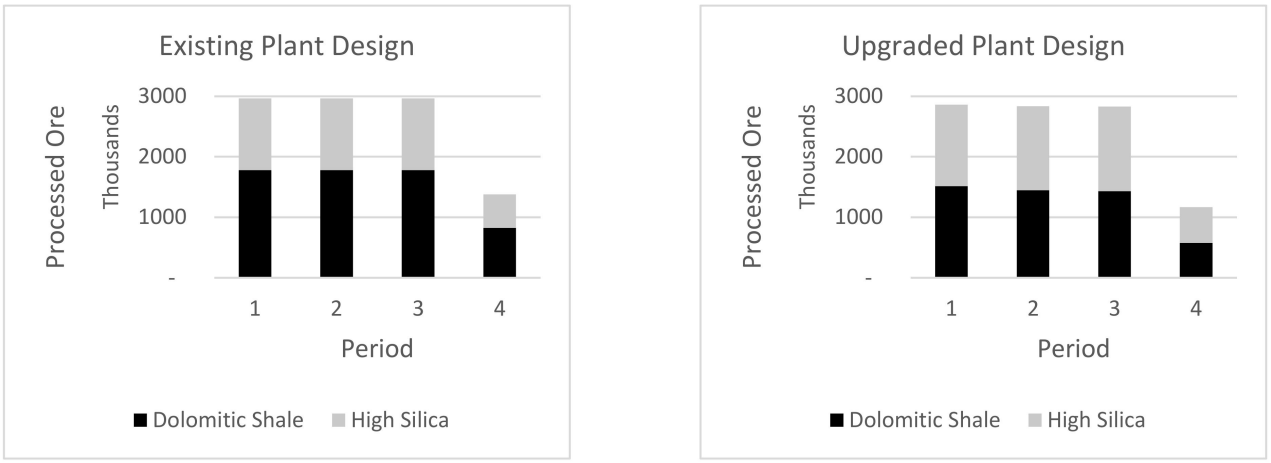

(**a**) (**b**)

Figure 5. Tonnes of ore processed per period for the existing (**a**) and upgraded (**b**) designs.

Figure 7a presents schematic views of the mine plan associated with the existing and updated plant designs. For the existing plant, its only operational mode restricts the mine plan by requiring as much ore as possible, which is particularly noticed in periods 1 and 2 and leads to a skewed pit design (Figure 7a). Conversely, the updated design allows the mine plan to extract the ore more evenly across the periods, observed mainly in periods 2 and 3 (Figure 7b). Similarly, to an observation made by Navarra et al. [17]: Figure 7 shows visual confirmation that the strategic mine plan and the metallurgical plant design are coupled, and should therefore be evaluated simultaneously, within the same computational framework. Furthermore, the feed blending is inevitably coupled with the plant design and strategic mine plan.

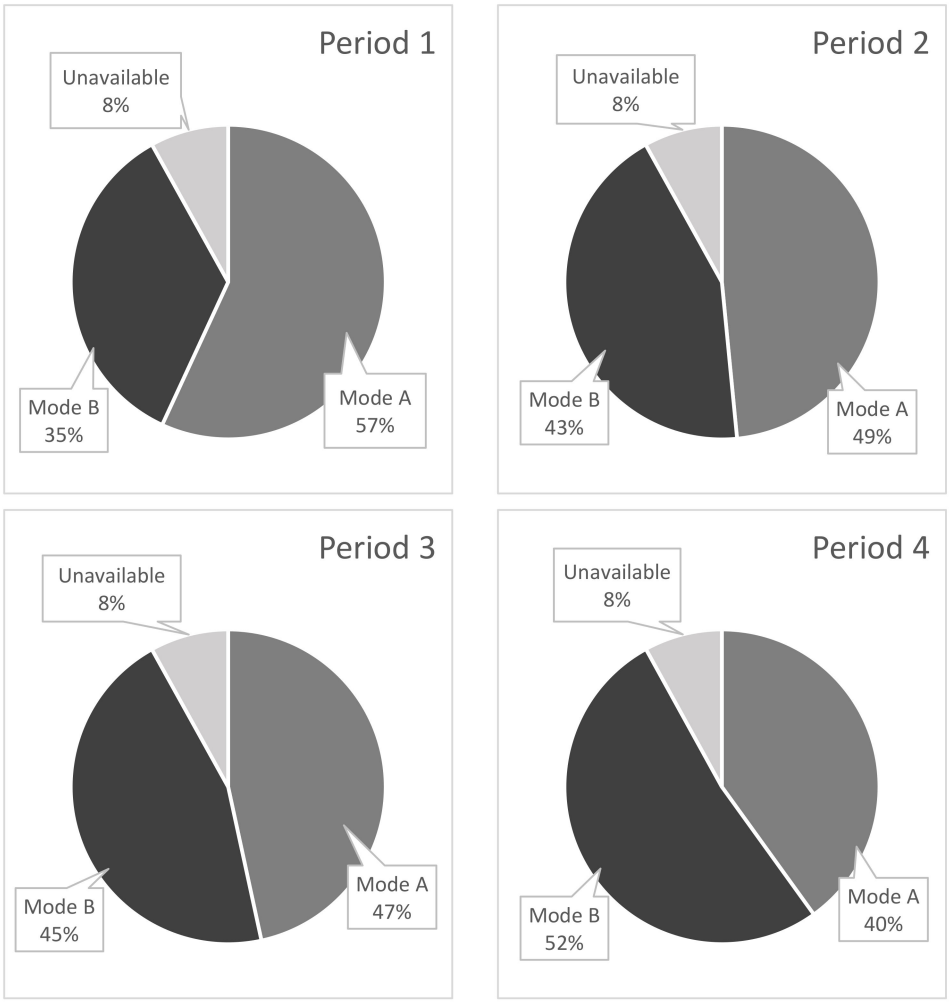

Figure 6. Time distribution of plant operating mode for the upgraded plant.

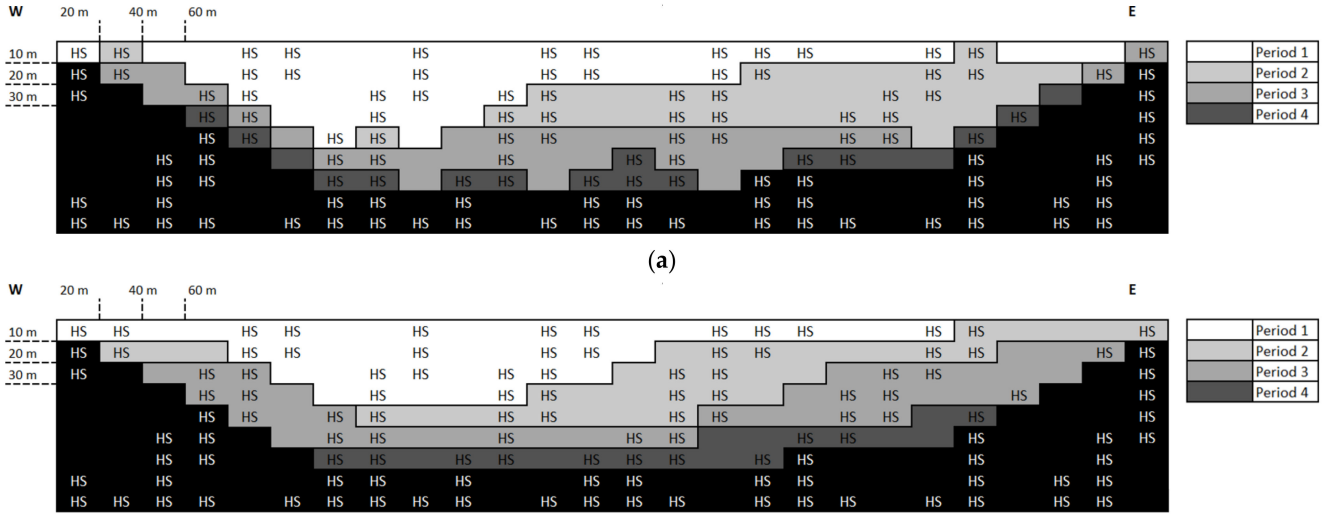

Figure 7. Schematic view of mine plan (XZ-planar cut along middle Y value) associated with the existing (**a**) and upgraded plant designs (**b**). HS: high silica blocks.

5. Conclusions

This work presented the selection of a metallurgy plant design that maximizes the cumulative NPV throughout the life of the mine, dealing with different ore types and geological uncertainty. This objective is reached by optimizing the mine plan under different metallurgical plant designs (hence different operational modes and feed blends). In particular, the sample calculations showed a case in which a potential upgrade would ensure a more balanced development of an open pit, which would diminish the amount of mining equipment. This more balanced development required an additional degree of freedom, as manifested by a second operating mode that was represented within the optimization framework. Furthermore, this optimization framework runs a paralyzed algorithm based on a VND metaheuristic to determine the periods where the blocks are extracted and embedded linear programs to deal with the mass balancing required by the plant's operational modes. This level of detail had not been possible in the previous development of the VND algorithm [16–18] and is essential for designing or redesigning metallurgical plants [15], which depend on short-term decisions regarding blending.

The authors consider this study a successful step in narrowing the gap between the mine and plant and, therefore, reaching a holistic view shared by multidisciplinary roles inside mining companies. In establishing the context for the sample computations, the grindability of the ore was considered a critical geometallurgical attribute, as represented by the Bond Work Index. However, the authors acknowledge the need for more experimentation to measure accurately the impact of considering operational modes to react simultaneously to different ore types and grade uncertainty. Among these experiments, it is desirable for an efficient implementation of Equation (11) so that the modes may support composition ranges and consider additional features such as strategic stockpiles, multiple processing streams and market uncertainty. In developing applied case studies (similar to the one in Section 4 of this paper), more computational experiments can be conducted in tandem with laboratory-scale metallurgical analyses, to establish and potentially extend the operability of a proposed plant. Moreover, in light of current trends, there is an interest to relate our methods to the carbon footprint of a mine, as well as other environmental impacts concerning tailings treatment and water conservation. It is our hope that the paper can stimulate other researchers and mine developers to test our methods for their specific mining operations.

Author Contributions: Conceptualization, A.Q., J.Ó., R.A. and A.N.; methodology, A.Q. and A.N.; software, A.Q.; validation, A.Q., J.Ó. and A.N.; investigation, A.Q., R.A. and J.Ó.; resources, A.Q.; data curation, A.Q. and J.Ó.; writing—original draft preparation, A.Q.; writing—review and editing, J.Ó. and A.N.; supervision, A.N.; funding acquisition, A.Q. and A.N. All authors have read and agreed to the published version of the manuscript.

Funding: This research was partially funded by a scholarship granted by the Chilean National Agency for Research and Development—ANID, grant number 72200205.

Data Availability Statement: The data presented in this study are available on request from the corresponding author. The data are not publicly available due to privacy concerns of anonymous industrial partners.

Acknowledgments: Powered@NLHPC: This research was partially supported by the supercomputing infrastructure of the NLHPC (ECM-02).

Conflicts of Interest: The authors declare no conflict of interest.

Appendix A

The Dantzig-Wolfe (DW) decomposition was proposed by Dantzig and Wolfe [47,48] and since then has become an important method for approaching linear programming problems whose constraints follow the structure presented in Figure A1, which is known as the block angular structure.

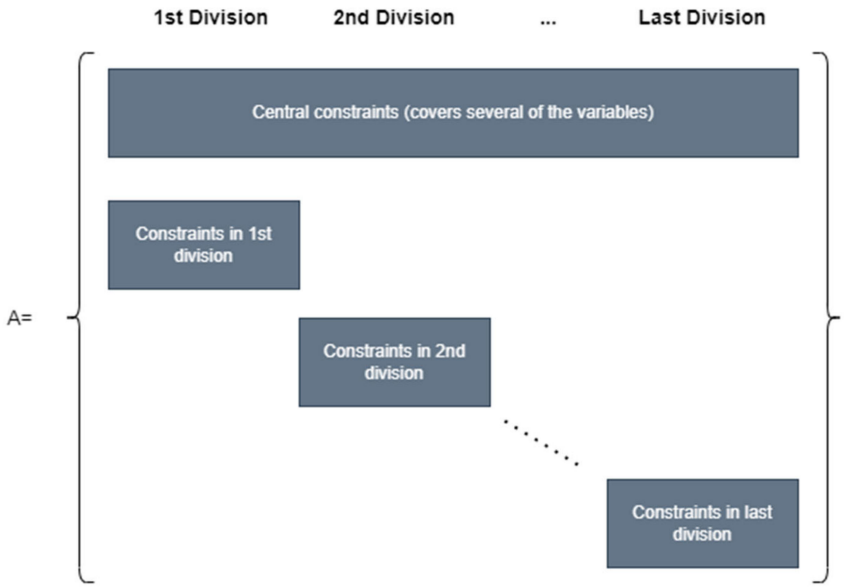

Figure A1. Block angular structure of constraints to apply DW decomposition.

The generic problem to be solved is defined as:

$$\max cx \tag{A1}$$

Subject to

$$Ax \leq b,\ x \geq 0 \tag{A2}$$

The A matrix has the block angular structure, where A_i (i = 1, 2, ..., 2N) are matrices, and the 0s are null matrices.

$$A = \begin{bmatrix} A_1 & A_2 & \dots & A_N \\ A_{N+1} & 0 & \dots & 0 \\ 0 & A_{N+2} & \dots & 0 \\ \vdots & \vdots & \ddots & \vdots \\ 0 & 0 & \dots & A_{2N} \end{bmatrix} \tag{A3}$$

Based on these definitions, the problem can be rewritten as:

$$\max \sum_{j=1}^{N} c_j x_j \tag{A4}$$

Subject to

$$[A_1, A_2, \dots, A_N, I] \begin{bmatrix} x \\ x_s \end{bmatrix} = b_0,\ \begin{bmatrix} x \\ x_s \end{bmatrix} \geq 0 \tag{A5}$$

$$A_{N+j} x_j \leq b_j \ and \ x_j \geq 0,\ for\ j = \{1, 2, \dots, N\} \tag{A6}$$

where c_j, x_j, b_0, and b_j are vectors such that c = [c_1, c_2, . . . , c_N], x^T = [x_1, x_2, . . . , x_N], b^T = [b_0, b_1, . . . , b_N], and x_s is the vector of slack variables for the first set of constraints.

The set of points x_j, such that $x_j \geq 0$ and $A_{N+j} x_j \leq b_j$, constitutes a convex set with a finite number of extreme points. Under the assumption that the set is bounded, any point in the set can be represented as a convex combination of the extreme points. If n_j is the number of extreme points, these points are denoted by x^*_{jk} for k = 1, 2, . . . , n_b

$$x_j = \sum_{k=1}^{n_j} \rho_{jk} x^*_{jk} \tag{A7}$$

$$\sum_{k=1}^{n_j} \rho_{jk} = 1, \ \ \rho_{jk} \geq 0 \tag{A8}$$

Therefore, this formulation provides a method for representing the feasible solutions to subproblem j without using any original constraints. The overall (master) problem is restated as the following:

$$\max \sum_{j=1}^{N} \sum_{k=1}^{n_j} (c_j x_{jk}^*) \rho_{jk} \tag{A9}$$

Subject to

$$\sum_{j=1}^{N} \sum_{k=1}^{n_j} (A_j x_{jk}^* (\rho_{jk} + x_s = b_0, \ \ x_s \geq 0 \ for \ j = \{1, 2, \ldots N\} \tag{A10}$$

$$\sum_{k=1}^{n_j} \rho_{jk} = 1 \ and \ \rho_{jk} \geq 0, \ \ for \ j = \{1, 2, \ldots, N\} \tag{A11}$$

Let B be the current basis matrix and let c_B be the corresponding vector of basic variables coefficients in the objective function. Let m_0 denote the number of elements of b_o. Let $(B^{-1})_{1;m_0}$ be the matrix consisting of the first m_0 columns of B^{-1}, and let $(B^{-1})_i$ be the vector consisting of the i^{th} column of B^{-1}. Then the subproblems are defined as the following:

$$\min(c_B(B^{-1}(_{1;m_0} A_j - c_j(x_j + c_B \left(B^{-1} \right)_{m_0 + j} \tag{A12}$$

Subject to

$$A_{N+j} x_j \leq b_j, \ \ x_j \geq 0 \tag{A13}$$

The decomposition is applied to the linear program presented in Equations (5)–(10) by changing the variables as stated in Equations (A14) and (A15). If two operational modes are considered, it is observed that each subproblem has a feasible region delimitated by points x_{b1}^* (0,0)—meaning that the block has not been processed; x_{b2}^*(1,0)—block entirely processed by mode A; and x_{b3}^*(0,1) block processed by mode B (Figure A2). This provides a better comprehension of the nature of the problem.

$$\sum_{o \in \mathcal{O}} \frac{m_{bso}}{m_b} = \sum_{k=1}^{3} \rho_{bk} x_{bk}^* \tag{A14}$$

$$\sum_{k=1}^{3} \rho_{bk} = 1 \ and \ \rho_{bk} \geq 0 \tag{A15}$$

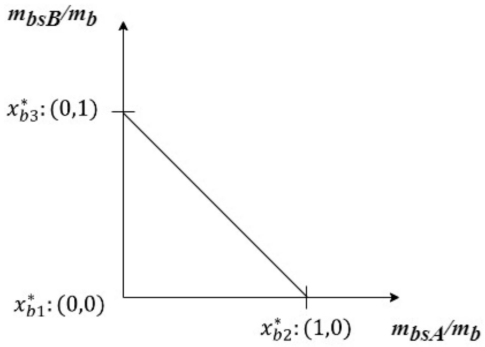

Figure A2. Feasible region of each subproblem.

In the case of a third mode, Figure A2 would be extended to consider a third dimension, coming out of the page, and Equations (A14) and (A15) would consider the four vertices

of a tetrahedron. More generally, for n modes, the structure of Equations (A14) and (A15) would be extended in consideration of the n vertices of an n-dimensional simplex.

To map the linear program presented in Equations (5)–(10) into the block angular structure of Figure A1, the central constraints are Equations (7) and (8), whereas the constraints within the block divisions correspond to Equation (6). Based on Equations (A14) and (A15), the linear program is reformulated as follows, where Equations (A17) and (A18) are Equations (7) and (8), and Equation (6) is transformed into Equation (A19):

$$\max \sum_{b \in \mathcal{B}_t} \sum_{k=1}^{3} v_{bso}(\rho_{bk} x^*_{bk}) \tag{A16}$$

Subject to

$$\sum_{b \in \mathcal{B}_t} \sum_{k=2}^{3} \frac{m_b}{r_k} \rho_{bk} \leq d_t, \ \ \forall r_k > 0 \tag{A17}$$

$$\sum_{b \in \mathcal{B}_{tp}} m_{bk} - w_{kp} \sum_{b \in \mathcal{B}_t} m_{bk} = 0, \ \forall k = \{1,2,3\}, \ \forall p \in \mathcal{P} \tag{A18}$$

$$\sum_{k=1}^{3} \rho_{bk} = 1, \ \ \forall b \in \mathcal{B}_t \tag{A19}$$

$$\rho_{jk} \geq 0, \ \ \forall b \in \mathcal{B}_t, \ \forall k = \{1,2,3\} \tag{A20}$$

In this transformation, the basis inversion B^{-1} is trivial because each block division (Figure A1) consists of only one Equation (6), i.e., the basis "matrix" is only a scalar. In addition, it is acknowledged the transformation would be more complicated with a range of compositions, as described by Equation (11); however, this is the subject of a forthcoming paper in which the context explicitly demands ranges in feed compositions.

In terms of execution time, the new formulation does not reduce the number of variables or constraints; however, the DW decomposition uses delayed column generation, which reduces the size of the matrices and, therefore, decreases the time dedicated to multiplication. Within the execution of the VND algorithm, as blocks are being moved between periods, the $n_T \cdot n_S$ instances of the linear programs (Equations (5)–(10)) are never reinitiated from scratch. When blocks are added to a period, the DW decomposition reoptimizes from the previous state, whereas when blocks are removed from a period, a dual problem formulation allows reoptimization. The efficiency of the algorithm depends on the implementation of these reoptimization operations.

References

1. Skyttner, L. *General Systems Theory–Ideas & Applications*; World Scientific Publishing Co. Pte. Ltd.: Singapore, 2001; pp. 45–101.
2. Lishchuk, V.; Pettersson, M. The mechanisms of decision-making when applying geometallurgical approach to the mining industry. *Miner. Econ.* **2021**, *34*, 71–80. [CrossRef]
3. Wei, Y.; Sandenbergh, R. Effects of grinding environment on the flotation of Rosh Pinah complex Pb/Zn ore. *Miner. Eng.* **2007**, *20*, 264–272. [CrossRef]
4. Nad, A.; Saramak, D. Comparative Analysis of the Strength Distribution for Irregular Particles of Carbonates, Shale and Sandstone Ore. *Minerals* **2018**, *8*, 37. [CrossRef]
5. Wang, C.; Nadolski, S.; Mejia, O.; Drozdiak, J.; Klein, B. Energy and Cost Comparisons of HPGR Based Circuits with the SABC Circuit Installed at the Huckleberry Mine. In Proceedings of the 45th Annual Canadian Mineral Processors Operators Conference, Ottawa, ON, Canada, 22–24 January 2013.
6. Lois-Morales, P.; Evans, C.; Weatherley, D. Analysis of the size–dependency of relevant mineralogical and textural characteristics to particles strength. *Miner. Eng.* **2022**, *184*, 107572. [CrossRef]
7. Fuerstenau, D. *Report US NRC Committee on Comminution and Energy Consumption*; National Materials Advisory Board, Commission on Sociotechnical Systems: Washington, DC, USA, 1981.
8. Bueno, M.; Foggiatto, B.; Lane, G. Geometallurgy Applied in Comminution to Minimize Design Risks. In Proceedings of the 6th International Conference on Autogenous Semi-autogenous Grinding and High-Pressure Grinding Roll Technology, Vancouver, BC, Canada, 25–28 September 2015; pp. 1–19.

9. Both, C.; Dimitrakopoulos, R. Integrating geometallurgical ball mill throughput predictions into short-term stochastic production scheduling in mining complexes. *Int. J. Min. Sci. Technol.* **2022**, *in press*. [CrossRef]
10. Flores, L. Hardness model and reconciliation of throughput models to plant results at Minera Escondida Ltda, Chile. *Tech. Bull. SGS Miner. Serv.* **2005**, *5*, 1–14.
11. Wills, B.; Finch, J. Chapter 5-Comminution. In *Wills' Mineral Processing Technology: An Introduction to the Practical Aspects of Ore Treatment and Mineral Recovery*, 8th ed.; Wills, B., Finch, J., Eds.; Butterworth-Heinemann: Oxford, UK, 2016; pp. 109–122.
12. Bond, F. *Crushing and Grinding Calculations*; Allis Chalmers Manufacturing Co.: Milwaukee, WI, USA, 1961.
13. Haffez, G. Correlation between work index and mechanical properties of some Saudi Ores. *Mater. Test.* **2012**, *54*, 108–112. [CrossRef]
14. Dimitrakopoulos, R. Stochastic Optimization for Strategic Mine Planning: A Decade of Developments. *J. Min. Sci.* **2011**, *47*, 138–150. [CrossRef]
15. Navarra, A.; Rafiei, A.; Waters, K. A system approach to mineral processing based on mathematical programming. *Can. Metall. Q.* **2017**, *56*, 35–44. [CrossRef]
16. Navarra, A.; Waters, K. Concentrator utilization under geological uncertainty. *Can. Metall. Q.* **2016**, *55*, 470–478. [CrossRef]
17. Navarra, A.; Menzies, A.; Jordens, A.; Waters, K. Strategic evaluation of concentrator operational modes under geological uncertainty. *Int. J. Miner.* **2017**, *164*, 45–55. [CrossRef]
18. Navarra, A.; Grammatikopoulos, T.; Waters, K. Incorporation of geometallurgical modelling into long-term production planning. *Miner. Eng.* **2018**, *120*, 118–126. [CrossRef]
19. Newman, A.; Rubio, E.; Caro, R.; Weintraub, A.; Eureke, K. A review of operations research in mining planning. *Interface* **2010**, *40*, 222–245. [CrossRef]
20. Tolouei, K.; Moosavi, E.; Tabrizi, A.; Afzal, P.; Bazzazi, A. An optimization approach for uncertainty-based long-term production scheduling in open-pit mines using meta-heuristic algorithms. *Int. J. Min. Reclam. Environ.* **2020**, *35*, 115–140. [CrossRef]
21. Lamghari, A.; Dimitrakopoulos, R.; Ferland, J. A variable neighborhood descend algorithm for an open-pit mine production scheduling problem with metal uncertainty. *J. Oper. Res. Soc.* **2014**, *65*, 1305–1314. [CrossRef]
22. Dimitrakopoulos, R. (Ed.) Stochastic Mine Planning–Methods, Examples and Value in an Uncertain World. In *Advances in Applied Strategic Mine Planning*; Springer: Cham, Switzerland, 2018; pp. 101–115.
23. Paravarzar, S.; Emery, X.; Madani, N. Comparing sequential Gaussian and turning bands algorithms for cosimulating grades in multi-element deposits. *Comptes Rendus Geosci.* **2015**, *347*, 84–93. [CrossRef]
24. Morales, N.; Nancel-Penard, P.; Espejo, N. Development and analysis of a methodology to generate operational open-pit mine ramp designs automatically. *Optim. Eng.* **2022**, *23*, 1573–2924. [CrossRef]
25. Nancel-Penard, P.; Morales, N.; Cornillier, F. A recursive time aggregation-disaggregation heuristic for the multidimensional and multiperiod precedence-constrained knapsack problem: An application to the open-pit mine block sequencing problem. *Eur. J. Oper. Res.* **2022**, *303*, 1088–1099. [CrossRef]
26. Deutsch, M.; Dagdelen, K.; Johnson, T. An Open-Source Program for Efficiently Computing Ultimate Pit Limits: MineFlow. *Nat. Resour. J.* **2022**, *31*, 1175–1187. [CrossRef]
27. Rivera-Letelier, O.; Espinoza, D.; Goycoolea, M.; Moreno, E.; Muñoz, G. Production Scheduling for Strategic Open Pit Mine Planning: A Mixed-Integer Programming Approach. *Oper. Res.* **2020**, *68*, 1425–1444. [CrossRef]
28. Ramazan, S.; Dimitrakopoulos, R. Production scheduling with uncertain supply: A new solution to the open pit mining problem. *Optim. Eng.* **2013**, *14*, 361–380. [CrossRef]
29. Montiel, L.; Dimitrakopoulos, R. Optimizing mining complexes with multiple processing and transportation alternatives. *Eur. J. Oper. Res.* **2015**, *247*, 166–178. [CrossRef]
30. Goodfellow, R.; Dimitrakopoulos, R. Global optimization of open pit mining complexes with uncertainty. *Appl. Soft Comput.* **2016**, *40*, 292–304. [CrossRef]
31. Saliva, Z.; Dimitrakopoulos, R. Simultaneous stochastic optimization of an open pit gold mining complex with supply and market uncertainty. *Int. J. Min. Sci. Technol.* **2019**, *128*, 216–229.
32. L'Heureux, G.; Gamache, M.; Soumis, F. Mixed integer programming model for short term planning in open-pit mines. *Int. J. Min. Sci. Technol.* **2013**, *122*, 101–109. [CrossRef]
33. Leite, A.; Dimitrakopoulos, R. Stochastic optimization model for open pit mine planning: Application and risk analysis at copper deposit. *Int. J. Min. Sci. Technol.* **2007**, *116*, 109–118.
34. Lamghari, A.; Dimitrakopoulos, R. A diversified Tabu Search approach for the open-pit mine production scheduling problem with metal uncertainty. *Eur. J. Oper. Res.* **2012**, *222*, 642–652. [CrossRef]
35. Kan, A. Long-term production scheduling of open pit mines using particle swarm and bat algorithms under grade uncertainty. *J. S. Afr. Inst. Min. Metall.* **2018**, *118*, 361–368. [CrossRef]
36. Muñoz, G.; Espinoza, D.; Goycoolea, M.; Moreno, E.; Queyranne, M.; Rivera, O. A study of the Bienstock-Zuckerberg algorithm: Applications in mining and resource constrained project scheduling. *Comput. Optim. Appl.* **2018**, *69*, 501–534. [CrossRef]
37. Lamghari, A.; Dimitrakopoulos, R.; Ferland, J. A hybrid method based on linear programming and variable neighborhood descent for scheduling production in open-pit mines. *J. Glob. Optim.* **2015**, *65*, 555–582. [CrossRef]
38. Pease, J.; Curry, D.; Young, M. Designing flotation circuits for high fines recovery. *Miner Eng.* **2006**, *19*, 831–840. [CrossRef]

39. Leach, D.; Bradley, D.; Huston, D.; Pisarevsky, S.; Taylor, R.; Gardoll, S. Sediment-hosted lead-zinc deposits in Earth history. *Econ. Geol.* **2010**, *105*, 593–625. [CrossRef]
40. Neumann, N.L.; Southgate, P.N.; Gibson, G.M. Defining unconformities in Proterozoic sedimentary basins using detrital geochronology and basin analysis—An example from the Mount Isa inlier, Australia. *Precambrian Res.* **2009**, *168*, 149–166. [CrossRef]
41. Page, R.W.; Jackson, M.J.; Krassay, A.A. Constraining sequence stratigraphy in north Australia basins: SHRIMP U-Pb zircon geochronology between Mt. Isa and McArthur River. *Aust. J. Earth Sci.* **2000**, *47*, 431–460. [CrossRef]
42. Large, R.R.; Bull, S.W.; McGoldrick, P.J.; Derrick, G.; Carr, G.; Walters, S. Stratiform and strata-bound Zn-Pb-Ag deposits of the Proterozoic sedimentary basins of northern Australia. In *Economic Geology One Hundredth Anniversary Volume*; Hedenquist, J.W., Thompson, J.F.H., Goldfarb, R.J., Richards, J.P., Eds.; Society of Economic Geologists: Littleton, CO, USA, 2005; pp. 931–963.
43. Davis, T. Mine-scale structural controls on the Mount Isa Zn-Pb-Ag and Cu orebodies. *Econ. Geol.* **2004**, *99*, 543–559. [CrossRef]
44. Perkins, W.G. Mount Isa silica dolomite and copper orebodies; the result of a syntectonic hydrothermal alteration system. *Econ. Geol.* **1984**, *79*, 601–637. [CrossRef]
45. Cave, B.; Richard Lilly, R.; Barovich, K. Textural and geochemical analysis of chalcopyrite, galena and sphalerite across the Mount Isa Cu to Pb-Zn transition: Implications for a zoned Cu-Pb-Zn system. *Ore Geol. Rev.* **2020**, *124*, 103647. [CrossRef]
46. Neudert, M. A Depositional Model for the Upper Mount Isa Group and Implications for Ore Formation. Ph.D. Thesis, Australian National University, Canberra, Australia, May 1983.
47. Dantzig, G.; Wolfe, P. Decomposition Principle for Linear Programs. *Oper. Res.* **1960**, *8*, 101–111. [CrossRef]
48. Hillier, F.; Lieberman, G. *Introduction to Operations Research*; McGraw-Hill Education: New York, NY, USA, 2015; pp. 1186–1198.